Journal of Structural Geology 33 (2011) 192–202

Contents lists available at ScienceDirect

Journal of Structural Geology

journal homepage: www.elsevier.com/locate/jsg

Deformation partitioning in transpressional shear zones with an along-strike stretch component: An example from the Superior Boundary Zone, Manitoba, Canada

Yvette D. Kuiper [a,*], Shoufa Lin [b,c], Dazhi Jiang [d]

[a] Department of Geology and Geophysics, Boston College, Chestnut Hill, MA 02467, USA
[b] Department of Earth Sciences and Environmental Sciences, University of Waterloo, Waterloo, Ontario N2L 3G1, Canada
[c] School of Resource and Environmental Engineering, Hefei University of Technology, Hefei 230009, PR China
[d] Department of Earth Sciences, University of Western Ontario, London, Ontario N6A 5B7, Canada

ARTICLE INFO

Article history:
Received 5 February 2010
Received in revised form
27 June 2010
Accepted 4 July 2010
Available online 14 July 2010

Keywords:
High-strain zone
Strain partitioning
Triclinic flow
Orogen-parallel stretch
Lineation
Trans-Hudson orogen

ABSTRACT

The partitioning of triclinic flow into domains of apparent monoclinic and apparent orthorhombic flow is described and discussed, using the Aiken River shear zone (ARSZ) as an example. The ARSZ is a 1–1.5 km wide east–west trending, dextral, north-side-up, mylonite zone, within the northern part of the Superior Province in Manitoba. It displays a high along-strike stretch (~10), which is most likely indicative of an escape-tectonic setting.

Although the central mylonite zone exhibits an apparent monoclinic fabric symmetry, the actual flow field was probably triclinic with a high simple shearing over pure shearing ratio, which resolves potential strain compatibility problems with neighbouring domains. The simple shearing-dominated zone is relatively narrow and has well-defined boundaries. An up to ~20 km wide zone adjacent to the ARSZ shows an apparent orthorhombic fabric symmetry with shear zone boundary-parallel horizontal stretch and shear zone-orthogonal shortening. However, the actual flow may have been triclinic with a low simple shearing over pure shearing ratio. Either way, the pure shear component of the ARSZ is distributed over a much broader area than the simple shear component and has diffuse boundaries. This is consistent with simple shearing being a softening and pure shearing a hardening process.

1. Introduction

Shear zones may have monoclinic or triclinic symmetry. Monoclinic shear zones can be considered as special cases, where the shear direction is parallel to one of the principal axes of the pure shearing component (cf. Robin and Cruden, 1994; Jiang and Williams, 1998; Lin et al., 1998). Shear zones may be thinning (transpression), thickening (transtension) or not changing thickness. Triclinic transpression zones are most common, because most orogens, active convergent plate boundaries, and volcanic arcs are associated with oblique convergence between plates or blocks (Jiang et al., 2001; Jiang, 2007b, and references therein).

In transpression zones, the shear zone-parallel maximum stretch is usually assumed or interpreted as being vertical or down dip (Sanderson and Marchini, 1984; Tikoff and Greene, 1997; Lin et al., 1998) or oblique (Czeck and Hudleston, 2003). Shear zone boundary-parallel horizontal stretch in subvertical shear zones is not commonly reported. Similarly, orogen-parallel stretch is not common and existing estimates of finite orogen-parallel stretch are low. The two types of stretch are related, because crustal-scale subvertical shear zones are generally parallel to the trend of the orogen. It is commonly believed that a high shear zone boundary-parallel horizontal stretch or orogen-parallel stretch is not favourable, because it would cause space and strain compatibility problems in deformation. Furthermore, strain hardening would resist the shear zone- or orogen-orthogonal (pure shear) shortening that usually occurs at the same time.

In this paper, we present evidence for a high shear zone boundary-parallel horizontal stretch in the subvertical Aiken River shear zone (ARSZ) in the Superior Boundary Zone, northeast of Thompson, Manitoba, Canada (Fig. 1). The amount of horizontal stretch along the shear zone is estimated to be in the order of 10. We discuss the feasibility of such high shear zone-parallel stretches, for the ARSZ, as well as in general. A common tectonic

* Corresponding author. Tel.: +1 617 552 3647; fax: +1 617 552 2462.
E-mail address: kuipery@bc.edu (Y.D. Kuiper).

0191-8141/$ – see front matter © 2010 Elsevier Ltd. All rights reserved.
doi:10.1016/j.jsg.2010.07.003

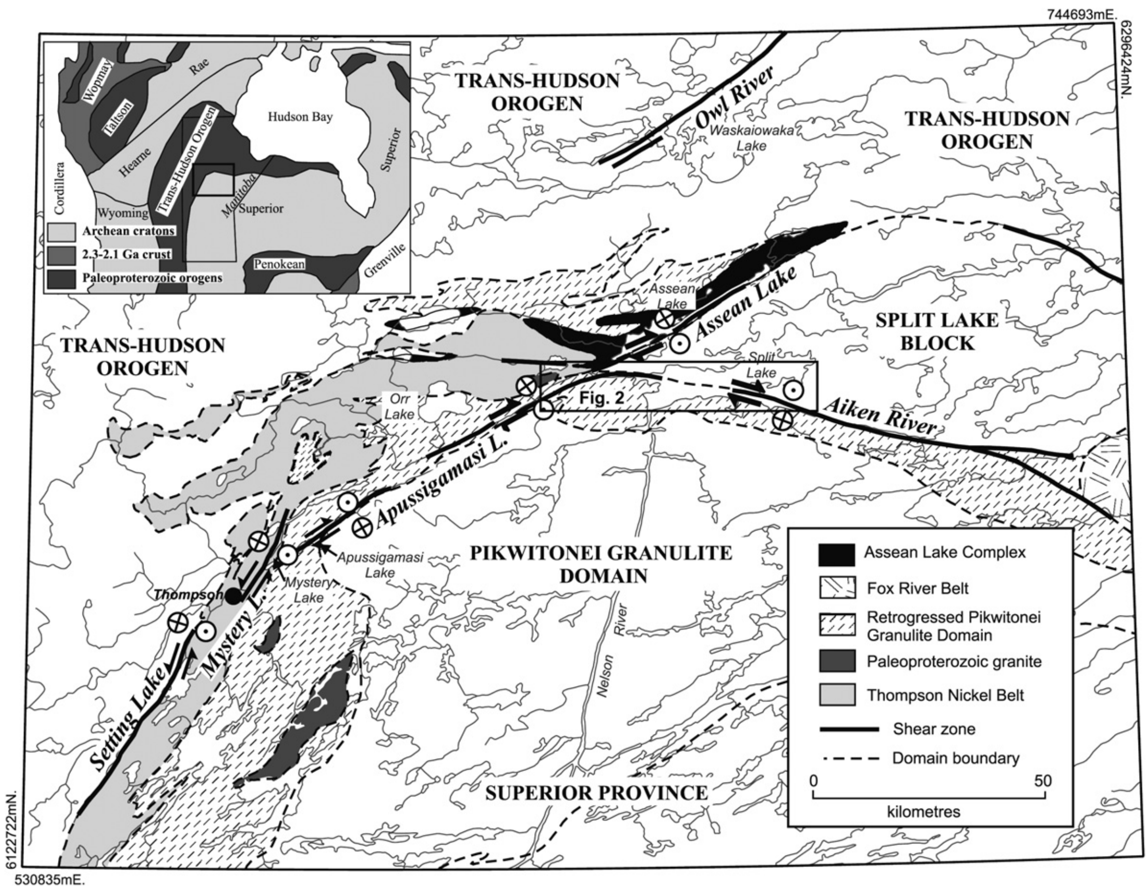

Fig. 1. Simplified geologic map of the northwestern Superior Boundary Zone (after Böhm et al., 2007). Shear zones and their senses of movement are indicated. Insert: simplified geological map of part of North America, showing Archean provinces and Paleoproterozoic belts.

setting for such shear zones may be lateral extrusion zones in escape-tectonic settings.

We also discuss strain partitioning in shear zones, using the ARSZ as an example. Transpression along this shear zone is partitioned into zones with a high and a low simple shearing over pure shearing ($\dot{\gamma}/\dot{\varepsilon}$) ratio, where 'simple shearing' and 'pure shearing' indicate rates of simple shear and pure shear, respectively (Means, 1990). The pure shear component is consistently distributed over a wider area than the simple shear component (cf. Lin et al., 1998), as is indicated by rotation patterns of lineations and fold hinge lines along the ARSZ, as well as by rotation or shear zone-orthogonal shortening or map scale structures along other shear zones in the Superior Boundary Zone (cf. Kuiper et al., 2009). Furthermore, triclinic flow along the ARSZ is partitioned into apparent monoclinic and apparent orthorhombic domains. The nature of these domains, and whether flow fields in these domains were truly monoclinic and orthorhombic, or triclinic with apparent monoclinic and orthorhombic symmetries, is discussed. It is argued that the domain with apparent monoclinic fabric symmetry is in fact a region of triclinic flow, based on strain compatibility arguments with adjacent domains. The apparent monoclinic fabric symmetry is a result of a high $\dot{\gamma}/\dot{\varepsilon}$ ratio and low finite strain. The domain with apparent orthorhombic fabric may be truly orthorhombic, or triclinic with a low $\dot{\gamma}/\dot{\varepsilon}$ ratio.

2. Geological background

The Superior Boundary Zone exists between the Archean Superior Province to the southeast and the Paleoproterozoic Trans-Hudson Orogen to the northwest. The Trans-Hudson Orogen is an amphibolite grade Paleoproterozoic belt that consists of Paleoproterozoic volcanic arc and passive margin sedimentary rocks, which record Paleoproterozoic continent collision and orogenesis (Machado, 1990; Ansdell, 2005; Corrigan et al., 2005). The Superior Province consists of Eoarchean to Neoarchean terranes that were amalgamated in the Neoarchean (Percival, 2007). The Pikwitonei Granulite Domain represents a mid- to deep crustal segment of the Superior Province. It consists of predominantly tonalitic and granodioritic gneisses that underwent granulite facies metamorphism and retrograde amphibolite grade metamorphism in the Neoarchean (Mezger et al., 1990; Böhm et al., 1999, 2007). The Split Lake Block consists of >2708 Ma gneisses and can be correlated with the Pikwitonei Granulite Domain (Corkery, 1985; Böhm et al., 1999; Kuiper et al., 2003, 2004a,b). It is bounded by the Assean Lake and Aiken River shear zones (Fig. 1). It consists of predominantly tonalitic and granodioritic gneisses with lower volumes of anorthosite, gabbroic and granitic gneisses, mafic granulite, layered amphibolite and pelitic schist and gneiss (Haugh, 1969; Corkery, 1985; Hartlaub et al., 2004). The Split Lake Block underwent granulite facies metamorphism and later amphibolite facies metamorphism, both in the Neoarchean (Corkery, 1985; Böhm et al., 1999, 2007; Downey et al., 2009).

The Assean Lake Complex (Fig. 1) consists of granitic and tonalitic gneiss, metasedimentary rocks and layered amphibolite that are older than 3.0 Ga material (Böhm et al., 2000, 2003, 2007; Hartlaub et al., 2006). The peak of metamorphism reached amphibolite facies. The Assean Lake Complex was deformed and metamorphosed during the Paleoproterozoic Trans-Hudson orogeny, but evidence for earlier events in the Late Archean and earliest Paleoproterozoic exist (Böhm et al., 1999, 2003). The Thompson Nickel Belt (Fig. 1) consists of Neoarchean gneisses (Machado et al., 1990; Böhm et al., 2007) and Paleoproterozoic supracrustal (Zwanzig, 2005; Zwanzig et al., 2007) and ultramafic (Hulbert et al., 2005) rocks, and is characterized by retrograde metamorphism.

Shear zones between the crustal blocks, described in more detail in Kuiper et al. (in review), display localized mylonite zones, but also show evidence for shortening across the shear zone, within the shear zone as well as in adjacent domains. Below, the ARSZ and adjacent structural domains are described and discussed in detail.

3. Aiken River shear zone and Split Lake Block

The geology related to the ARSZ has been divided into structural domains as follows (numbers correspond with domain numbers indicated in Fig. 2): (1) northern Pikwitonei Granulite Domain, (2) northern Pikwitonei Granulite Domain with refolded folds, (3) mylonite, (4) transitional zone, (5) southern Split Lake Block, and (6) central Split Lake Block. The structural domains are described below, from north to south (domains 6 to 1) and are summarized in Table 1.

3.1. Central Split Lake Block (domain 6)

The main structural pattern of rocks in the studied part of the central Split Lake Block is dominated by generally weakly deformed rocks (Fig. 3a) and generally moderately to steeply SE-plunging open to tight folds (Fig. 4a). The age of these folds is unknown, but they predate movement along the ARSZ. A spaced foliation (S_1) with strongly flattened rafts and felsic melt layers of up to several millimetres width exists in some of the gneisses. This foliation is folded tightly to isoclinally by the deformation that was responsible for the development of a penetrative gneissosity (S_2). This gneissosity is folded by the SE-plunging folds (F_3). An ~east–west trending vertical foliation (S_4) is present that appears axial-planar to the F_3 folds in the field. However, because the fold hinge lines and associated lineations do not lie in the plane of this foliation (see below), the foliation must be post-folding and may be related to movement along the ARSZ.

A moderately to steeply SE-plunging intersection lineation (L_3) is parallel to the F_3 fold hinge lines (Fig. 4a). The larger spread in orientations of fold hinge lines than that of lineations is attributed to the larger measurement error on fold hinge lines (especially for open folds) compared to that on lineations. The poles to S_2 form a weak girdle, the pole of which coincides with the concentration in the plunges of lineations and fold hinge lines to the southeast (Fig. 4a). The majority of S_2 surfaces dips steeply southeast, consistent with a generally open cylindrical geometry of the folds.

3.2. Southern Split Lake Block (domain 5)

Open to tight F_3 folds in domain 5 generally plunge shallowly east but can vary (Figs. 3b and 4b). The nature of the lineations was not always clear from field observations, but they are thought to be

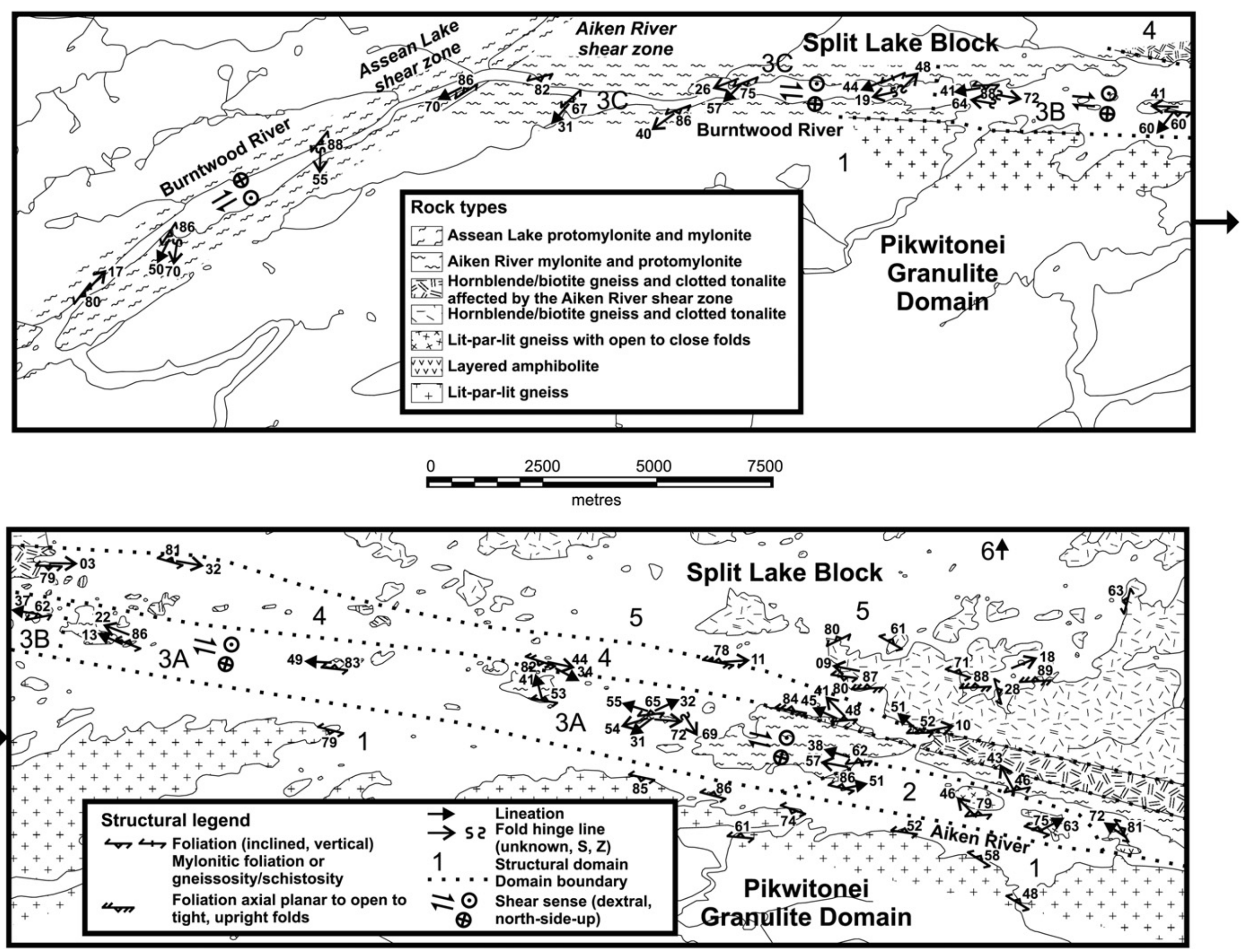

Fig. 2. Simplified geology of the Aiken River shear zone.

Table 1
Summary of structures and interpretation of Paleoproterozoic deformation in domains 3–6. ARSZ: Aiken River shear zone.

Domain	D1	D2	D3	D4	Dominant Paleoproterozoic syn-ARSZ deformation	Apparent Paleoproterozoic flow symmetry
	Pre-ARSZ	Pre-ARSZ	Pre-ARSZ	syn-ARSZ (Paleoproterozoic)		
6	Spaced foliation	Gneissosity and tight to isoclinal folds	Open to tight, moderately to steeply SE-plunging upright folds	East–west trending foliation	Weak shear zone-orthogonal shortening and strike-parallel shear zone boundary stretch	Orthorhombic
5		Gneissosity and tight to isoclinal folds	Open to tight, shallowly east-plunging upright folds	East–west trending foliation	Shear zone-orthogonal shortening and strike-parallel shear zone boundary stretch	Orthorhombic
4		Gneissosity and tight to isoclinal folds	Tight to isoclinal, shallowly east and westplunging upright folds	East–west trending foliation; shear fabrics mostly on fold limbs; non-cylindrical folds	Strong shear zone-orthogonal shortening and strike-parallel shear zone boundary stretch; local dextral, north-side-up shear	Orthorhombic (locally monoclinic close to ARSZ)
3				East–west trending mylonitic foliation; penetrative dextral, north-side-up shear fabrics and sheath folds	Dextral, north-side-up shear	Monoclinic

parallel to the fold hinge lines and are thus interpreted as L_3. The poles to the gneissosity (S_2) spread evenly along a girdle (Fig. 4b), suggesting parallel (Ramsay class 1B) style folding. Contrary to domain 6, the S_4 foliation is apparently axial planar to the east-plunging folds (Fig. 4b), possibly due to reorientation of the F_3 folds and not necessarily because they formed at the same time. Similar to domain 6, the S_4 foliation may have developed during deformation along the ARSZ (see below).

3.3. Aiken River transitional zone (domain 4)

Compared to F_3 folds in domain 5, those in domain 4 are tighter (commonly isoclinal) and the fold hinge lines plunge shallowly east and west (Fig. 4c). An example is shown in Fig. 3c. The lineations are parallel to F_3 fold hinge lines and are interpreted as L_3. A foliation exists that appears to be axial planar to the F_3 fold. However, based on continuity with structures in domains 5 and 6 we interpret it as a later foliation (S_4) that may be related to ARSZ deformation. Poles to S_2 form a girdle perpendicular to the F_3 fold hinge lines. The majority of S_2 planes is subvertical and east trending, which is the orientation of the fold limbs and S_4 (Fig. 4c). This confirms that the F_3 folds are isoclinal. We interpret that they developed as open to tight folds as in domains 5 and 6 and were subsequently tightened by D_4 (ARSZ-related) deformation. Dextral, north-side-up shear sense indicators (D_4) are visible on both fold limbs, but not on the hinges. At one location (Fig. 3d), a dextral shear zone cuts off half of a fold hinge. At locations very close to the mylonite zone (domain 3), fold hinge lines rotate towards steeper plunges (Figs. 3e and 4d). They may be interpreted as immature non-cylindrical folds that are related to sheath fold formation within the shear zone.

3.4. Aiken River shear zone mylonite (domain 3)

The ARSZ is a 1–1.5 km wide shear zone, exposed along the Aiken and Burntwood rivers (domain 3 in Fig. 9). It consists of fine- to medium-grained, mostly granitic to granodioritic and locally mafic mylonite and protomylonite, and decimetre-scale layers of chloritic schist. Mylonite is derived from rocks of both the Split Lake Block and the Pikwitonei Granulite Domain. For consistency with domains 4–6, all ARSZ-related fabrics are denoted D_4, even though earlier fabrics are so strongly overprinted that they are not recognizable any longer. Dextral, north-side-up movement is indicated by shear bands, S-C fabric, oblique foliation, asymmetric clasts (Fig. 5), and Z-folds. Locally, dextral fabric and lineations are folded by Z-folds, indicating that new Z-folds continued to develop during late shearing. A few north-side-up, dextral sheath folds exist (Fig. 3f). Complex fold patterns exist in the eastern part of the study area, perhaps because folds of the Split Lake Block (and Pikwitonei Granulite Domain?) were refolded by shear zone-related drag folds and/or sheath folds. The presence of shear bands and absence of kink structures, and the fact that fold hinge lines lie within the plane of the shear zone, indicate that the shear zone is thinning or transpressional (Williams and Price, 1990; Jiang and Williams, 1999; Kuiper et al., 2007).

The ARSZ generally dips steeply to the NNE (domain 3A, Figs. 6a and 9). Lineations plunge moderately to the WNW (Fig. 6b). Z-fold hinge lines spread along the plane of the foliation. S-folds are rare. Their fold hinge lines plunge moderately to the WSW (Fig. 6c). Towards the west, towards the Assean Lake shear zone, structures are essentially the same as described above, except that the entire shear zone, including foliations, lineations and fold hinge lines, trends west (domain 3B, Figs. 6d and 9). This is also apparent in the westerly trend of Split Lake towards the Burntwood River, as opposed to the WNW trend of the Aiken River (Fig. 9). Lineations plunge moderately to the west. Sheath folds in this domain indicate north-side-up (dextral) movement. The S-fold in Fig. 6d is part of a north-side-up sheath fold. Within ~10 km of the Assean Lake shear zone, the Burntwood River still trends west, whereas the mylonitic foliation trends WSW, parallel to that of the Assean Lake shear zone (Figs. 6e and 9). Fold hinge lines and lineations lie within the plane of the foliations (domain 3C; Fig. 6e). Rare sheath folds indicate north-side-up, dextral movement. Lineations plunge moderately to the WSW. The ENE-trending segment of the Burntwood River, farther west again, is part of the dextral, southeast-side-up Assean Lake shear zone, which crosscuts the ARSZ (Fig. 9; Kuiper et al., 2004b).

3.5. Pikwitonei Granulite Domain (domains 1 and 2)

Domains 1 and 2 are structurally dominated by tight to isoclinal upright, ESE-plunging folds. Domain 2 is a local area where these folds are refolded by steeply north-plunging open to close folds. Such refolded folds did not occur in domain 1 or elsewhere. Because this paper focuses on the north side of the ARSZ and southern Split Lake Block, domains 1 and 2 are not considered further in this paper. Detailed descriptions can be found in Kuiper et al. (2003).

4. Deformation partitioning along the Aiken River shear zone

Southeast-plunging folds of domain 6 consistently become tighter, and fold hinge lines display shallower east and west plunges, towards the ARSZ (domains 5 and 4). The fact that tightening of folds

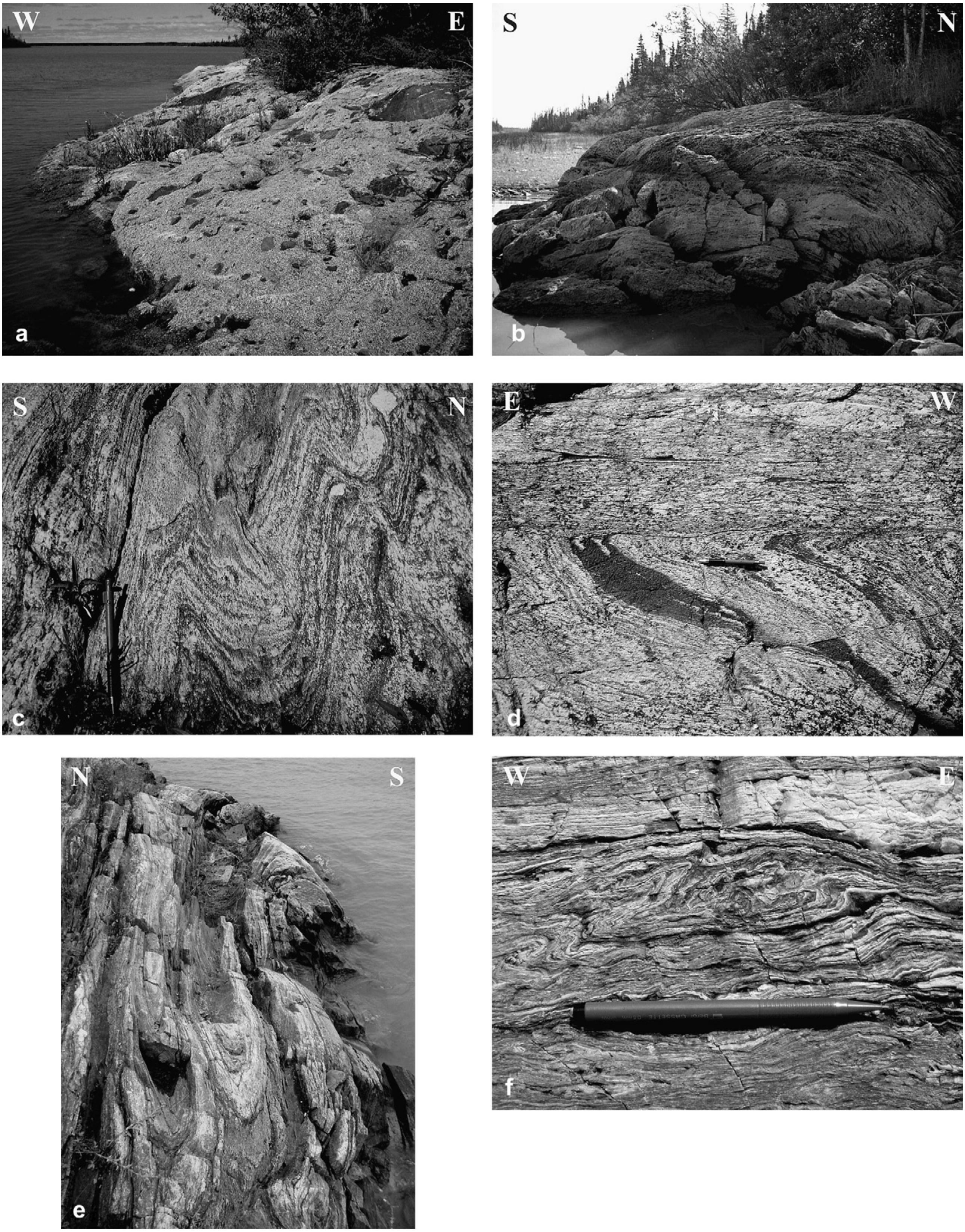

Fig. 3. Photographs of the rock types from the central Split Lake Block to the Aiken River shear zone: (a) weakly deformed (D_1) clotted tonalite (domains 5 and 6); (b) open east-plunging F_3 fold in hornblende/biotite gneiss (domain 5); (c) tight east-plunging F_3 folds in hornblende/biotite gneiss (apparently axial-planar S_4 foliation is parallel to the pencil (domain 4); (d) tightened F_3 fold hinge crosscut by dextral shear zone (domain 4); (e) rotation of F_3 fold hinge lines towards steeper orientations (steepening toward the front of the picture; domain 4); and (f) dextral, north-side-up D_4 sheath fold in mylonite (domain 3).

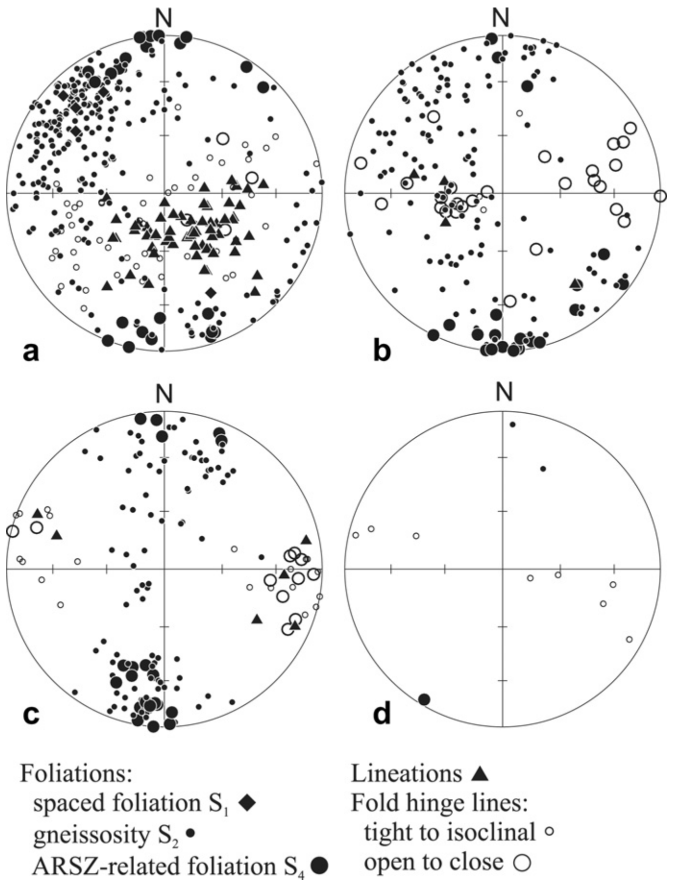

Fig. 4. Equal-area lower-hemisphere projections of structural data from the Split Lake Block: (a) central Split Lake Block (domain 6); (b) southern Split Lake Block (domain 5); (c) Aiken River transitional zone (domain 4), excluding station 609, where fold axes steepen; and (d) Aiken River transitional zone (domain 4), station 609. ARSZ is Aiken River shear zone.

in proximity to the shear zone occurs before shear sense indicators develop suggests that the pure shear component of the shear zone is accommodated in a wider zone than the simple shear component. This is consistent with conclusions drawn from the Roper Lake shear zone on Cape Breton Island, Canadian Appalachians by Lin et al. (1998), who discussed the phenomenon in more detail (see also Lin et al., 2007, and below). The plunge of the fold hinge lines becomes shallower towards the shear zone, suggesting shear zone boundary-parallel horizontal stretching. Therefore, the pure shear component of the shear zone includes shortening perpendicular to the shear zone and horizontal stretching parallel to it. The S_4 foliation in domain 6 is also interpreted as a result of shear zone-orthogonal shortening, implying that some shortening occurred as far as ~20 km north of the ARSZ.

In approaching the shear zone, dextral, north-side-up shear sense indicators develop on the limbs of the folds (domain 4). The shear sense is the same on both limbs and can thus not be attributed to shear on fold limbs because of folding. The fold hinges are not affected by shear, probably because shear deformation in a vertical plane can more easily be accommodated in the subvertical fold limbs than on the subhorizontal fold hinges. Closer to the mylonite zone, fold hinge lines start to rotate from subhorizontal to steeper orientations, perhaps as a result of shear in the shear zone. This rotation may be the initiation of sheath-fold development. Well-developed sheath folds are recognized within the mylonite zone to the west (domain 3C; Fig. 6e). Northeast-plunging Z-folds in the same domain may be immature folds that formed as a result of the same shear that was responsible for the development of sheath folds. Sheath folds in the ARSZ may either have developed from these shear zone-related folds or from the pre-existing folds described above.

Within the mylonite zone, dextral, north-side-up shear sense indicators are well developed and penetrative (Kuiper et al., 2003), and sheath folds are present. Shallowly east- and west-plunging folds (as in domain 4) are absent, as they have evolved into sheath folds and/or complex refolded folds. The simple shear component of the shear zone thus involves dextral, north-side-up movement.

4.1. Numerical models of rotation paths of pre-existing fold hinge lines

In summary, the transition from the moderately to steeply southeast-plunging folds of the Split Lake Block to shear zone-related structures displays the following phenomena as the shear zone is approached: (1) folds tighten and plunges change from moderately to steeply southeast to shallowly east (and west); (2) shear sense indicators develop on the fold limbs but not the fold hinges; (3) fold hinge lines become closer to the shear direction (the initiation of sheath fold development); and (4) dextral, north-side-up shear sense indicators are pervasive and sheath folds are present. The fold hinge line rotation towards subhorizontal orientations in domain 4 (phenomenon 1 above) cannot be a result of the dextral, north-side-up shear, because that would have steepened the pre-existing fold hinge lines. Because

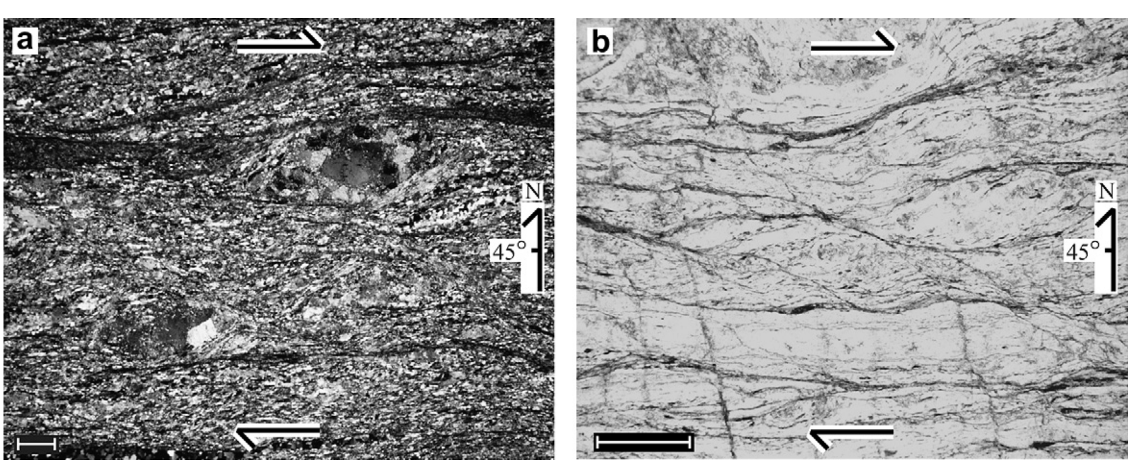

Fig. 5. (a) Sigma-clasts and S-C fabric (crossed nicols), and (b) S-C fabric and shear bands (C′ fabric) in plane polarised light, indicating dextral, north-side-up, shear along the Aiken River shear zone. Scale bars are 1 mm.

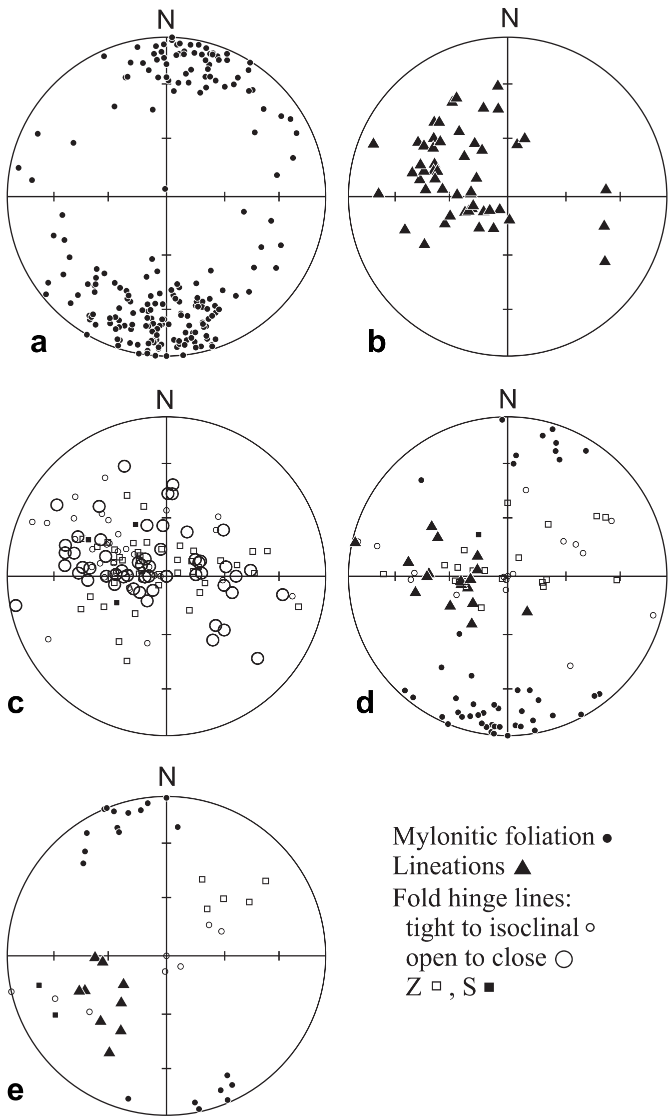

Fig. 6. Equal-area lower-hemisphere projections of D_4 structural data from mylonite of the Aiken River shear zone (domain 3), southeastern Split Lake: (a) foliations; (b) lineations; (c) fold hinge lines; (d) mylonite of western Split Lake; and (e) Aiken River shear zone mylonite along the Burntwood River.

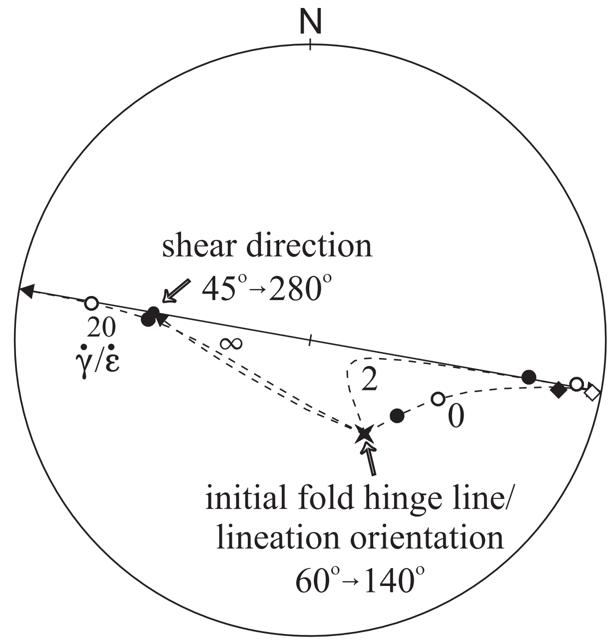

φ=45°	●	○	◆	◇
Stretch of fold hinge line				
$\dot{\gamma}/\dot{\varepsilon} = 20$:	5.3	11.3		
$\dot{\gamma}/\dot{\varepsilon} = 2$:	3.3	8.1		
$\dot{\gamma}/\dot{\varepsilon} = 0$:	1.0	1.1	3.2	13.9
Stretch along strike of shear zone				
$\dot{\gamma}/\dot{\varepsilon} = 20$:	2.1	4.5		
$\dot{\gamma}/\dot{\varepsilon} = 2$:	54.6	148.4		
$\dot{\gamma}/\dot{\varepsilon} = 0$:	1.4	2.1	9.5	42.5

Fig. 7. Rotation path of pre-existing fold hinge line or lineation, with initial orientation of 60° → 140° as in the Split Lake Block (domain 6), subjected to four different types of flow ($\dot{\gamma}/\dot{\varepsilon}$ ratios as indicated). The simple shear direction is 45° → 280°, as in the mylonite zone (domain 3). The maximum stretching direction of the pure shearing component is parallel to the strike of the shear zone boundary (00° → 280°) and the maximum shortening direction is perpendicular to the shear zone boundary (00° → 010°). Table shows stretch of the pre-existing fold hinge line or lineation and stretch along the strike of the shear zone boundary, for selected points along the rotation paths as indicated with symbols.

there is no evidence for any other simple shear, these rotations must be a result of pure shear. In a pure shear setting, linear fabrics rotate towards the maximum stretching direction (Jiang and Williams, 1998; Lin et al., 1998; Kuiper et al., 2007), which must therefore be subhorizontal and subparallel to the shear zone boundary. The shortening direction is interpreted as shear zone-normal and subhorizontal, based on the tightening of folds in domain 4 and the existence of shear bands in domains 4 and 3 (cf. Williams and Price, 1990). We interpret that at least part of the tightening of folds and fold hinge line rotation in domain 4 was coeval with movement along the ARSZ, because of the transitional nature of the structures in the two domains, and the exclusive existence of domain 4 structures in proximity of domain 3. Between domains 3 and 4, the simple shear component drops abruptly along the boundary between the two domains. Some simple shear is accommodated in localized zones close to the mylonite zone, in domain 4, for example along the fold limbs. Fig. 3d shows another example of localized simple shear in domain 4.

In order to constrain the potential deformation path within the various structural domains, we subjected the general orientation of fold hinge lines and lineations within the Split Lake Block (60° → 140°) to various types of flow. The general orientation of 60° → 140° was determined using a Gaussian density distribution function in the program SpheriStat on the lineation data in Fig. 4a. We did not use the fold hinge line data, because they are more scattered due to larger measurement errors than those for lineations, as explained in Section 3.1. While the exact orientations of the initial fold hinge lines and lineations vary, our models presented below are generally the same for any moderately to steeply southeast-plunging linear element. Four models of fold hinge line rotation in different types of flow are shown in Fig. 7: (1) simple shearing (monoclinic flow with $\dot{\gamma}/\dot{\varepsilon} = \infty$), (2) transpression (triclinic flow with $\dot{\gamma}/\dot{\varepsilon} = 20$ and 2), and (3) pure shearing (orthorhombic flow with $\dot{\gamma}/\dot{\varepsilon} = 0$). In the models, the simple shear direction is 45° → 280°, based on lineation and fold hinge line orientations within the mylonite zone. For the pure shearing component, the maximum stretching direction is parallel to the strike of the shear zone boundary (00° → 280°) and the maximum shortening direction is perpendicular to the shear zone boundary (00° → 010°). In our models, fold hinge lines and lineations are treated as material lines, as in Kuiper et al. (2007). A material line can be treated as a rigid prolate object with an aspect ratio of infinity. The rotation of rigid ellipsoidal objects in viscous flows is described by Jeffery's (1922) theory. To model the rotation of fold hinge lines we used the method and program of Jiang (2007a).

In the simple shearing model ($\dot{\gamma}/\dot{\varepsilon} = \infty$), pre-existing fold hinge lines rotate towards the shear direction. Monoclinic flow with the maximum stretching direction of the pure shearing component parallel to the shear direction would result in a similar rotation path, but since we have reason to believe that the maximum stretching direction is horizontal (see above), which would make the flow triclinic, we did not model monoclinic transpression.

For the triclinic models we used simple shearing and pure shearing components, as explained above, and varied the $\dot{\gamma}/\dot{\varepsilon}$ ratio. For $\dot{\gamma}/\dot{\varepsilon} = 20$, the rotation pattern for low strains is quite similar to that of simple shearing, but at high strains the fold hinge lines rotate through shallowly westerly plunging orientations to the maximum stretching direction of the pure shearing component (fabric attractor; 00° → 280°). With a higher pure shearing component, $\dot{\gamma}/\dot{\varepsilon} = 2$, the fold hinge lines first rotate towards steeper orientations and then through shallowly easterly plunging orientations to the fabric attractor (00° → 100°).

In the pure shearing model ($\dot{\gamma}/\dot{\varepsilon} = 0$), the maximum stretching direction is horizontal and parallel to the shear zone boundary and the maximum shortening direction is horizontal and perpendicular to the shear zone boundary, as above. Fold hinge lines rotate directly towards the maximum stretching direction (fabric attractor; 00° → 100°). Note that with only a small simple shearing component (e.g. $\dot{\gamma}/\dot{\varepsilon} = 2$, see above), the rotation path looks significantly different from the pure shearing rotation path.

4.2. Applications of models to structural domains along the Aiken River shear zone

Fold hinge lines and lineations rotate from 60° → 140° in the Split Lake Block to horizontal (00° → 280°) in domain 4 or the Aiken River transitional zone (Fig. 8a,b), which is consistent with the pure shear rotation path as presented above. Because no steepening of fold hinge lines is observed in domain 4 as in the triclinic and simple shear flow models, the simple shearing component must be very small or not present. Thus, the flow in domain 4 in proximity to the mylonite zone was pure shearing-dominated or approximately orthorhombic.

Fold hinge lines and lineations within the mylonite zone (domain 3) rotate towards the shear direction (45° → 280°; Fig. 8c), which appears to be consistent with a simple shear flow path (Fig. 7). Monoclinic transpression, either with the maximum stretching direction of the pure shearing component parallel to the shear direction, or with equal stretching in all directions parallel to the shear zone boundary, would result in a similar rotation path of the fold hinge lines and lineations as simple shearing. The fabric attractor would be parallel to the shear direction (cf. Jiang and Williams, 1998, 1999; Lin et al., 1998; Kuiper et al., 2007). However, we interpret the maximum stretching direction of the pure shearing component as being horizontal, consistent with domain 4, and therefore we prefer the simple shearing model over the monoclinic transpression models. Triclinic flow paths would, at high strains, result in rotation of the fold hinge lines and lineations towards horizontal orientations (Fig. 7), which is not observed. However, at low strains and high $\dot{\gamma}/\dot{\varepsilon}$ ratios (e.g. $\dot{\gamma}/\dot{\varepsilon} = 20$), the triclinic flow path is similar to the monoclinic flow path. Such a triclinic flow is the most likely interpretation for domain 3, as is discussed in detail below.

Some of the lineations within the mylonite zone (domain 3), may not have been pre-existing as assumed above, but may have formed as a result of the movement that was responsible for mylonitisation. For these newly formed stretching lineations, the models presented above do not apply. Jiang and Williams (1998) and Lin et al. (1998) modeled the orientations of the strain ellipsoid during various progressive deformations. Stretching lineations are approximated by the long axes of the strain ellipsoids, λ_1, and the poles to the foliations are the short axes of the strain ellipsoids, λ_3. Fig. 9a shows a model of rotation patterns for lineations in monoclinic flow, and Fig. 9b for triclinic flow, based on Jiang and Williams (1998) and Lin et al. (1998). The coordinate system is orientated so that the shear direction and sense, and the stretching and shortening directions of the pure shearing component, are the same as in the models presented above. In monoclinic flow (Fig. 9a), lineations rotate towards the shear direction, which is consistent with field results (Fig. 8c). In Fig. 9b, rotation paths of lineations for triclinic flow are indicated by the dashed lines for various $\dot{\gamma}/\dot{\varepsilon}$ ratios. For any $\dot{\gamma}/\dot{\varepsilon}$ ratio, lineations rotate towards horizontal during progressive deformation. In domain 3, subhorizontal lineations are not observed and therefore the orientations of lineations within the mylonite zone appear to be more consistent with monoclinic strain than with triclinic strain. However, as for pre-existing fold hinge lines and lineations, at low strains and high $\dot{\gamma}/\dot{\varepsilon}$ ratios (e.g. $\dot{\gamma}/\dot{\varepsilon} = 20$), the triclinic flow path for λ_1 is similar to its monoclinic flow path.

From the discussion above, it follows that fold hinge line and lineation orientations in the mylonite zone (domain 3) appear to be

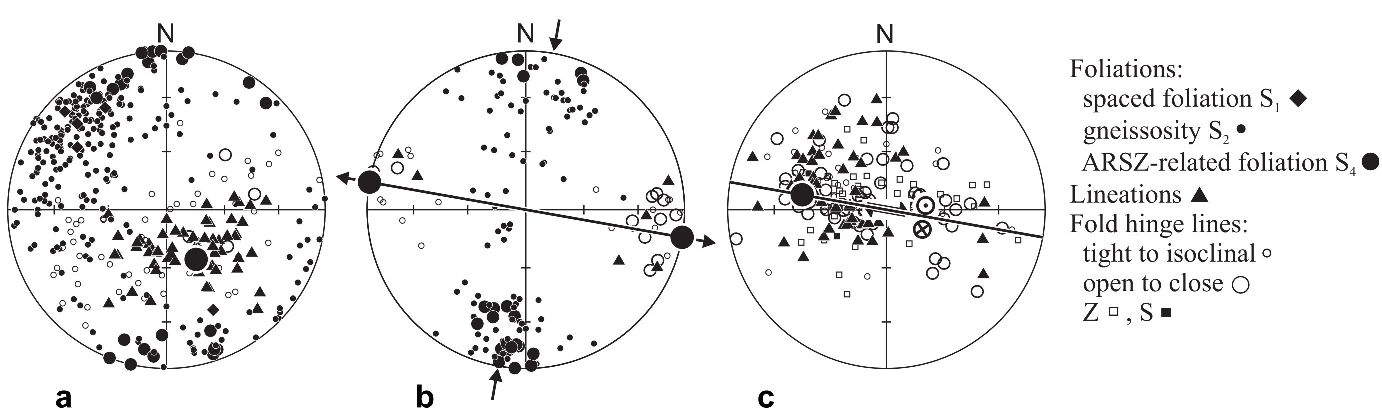

Fig. 8. Fabric attractors (largest filled circles) for (a) the Split Lake Block (domain 6), (b) the transitional domain (domain 4), which is dominated by pure shearing as indicated, and (c) the mylonite zone (domain 3), which is dominated by simple shearing as indicated. ARSZ is Aiken River shear zone.

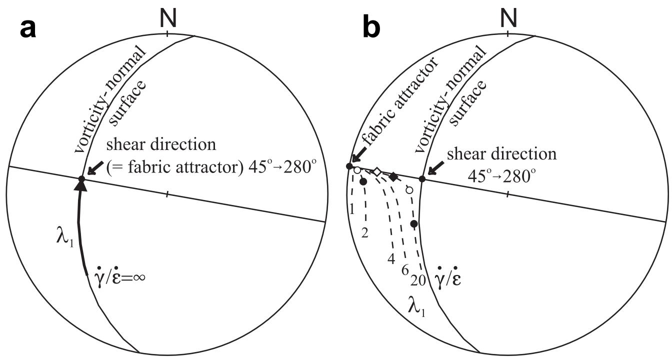

c

φ=45°	•	○	◆	◇
Stretch of lineation				
$\dot{\gamma}/\dot{\varepsilon} = 20$:	2.3	6.6	14.7	34.9
$\dot{\gamma}/\dot{\varepsilon} = 2$:	2.7	6.6		
Stretch along strike of shear zone				
$\dot{\gamma}/\dot{\varepsilon} = 20$:	1.1	1.4	2.2	4.8
$\dot{\gamma}/\dot{\varepsilon} = 2$:	2.3	5.4		
Strain intensity (Ramsay & Huber, 1983)				
$\dot{\gamma}/\dot{\varepsilon} = 20$:	1.9	9.5	30.7	115.9
$\dot{\gamma}/\dot{\varepsilon} = 2$:	3.3	12.2		

Fig. 9. Rotation path of lineation, or long axis of strain ellipsoid (λ_1) for simple shearing (a) and triclinic transpression (b) with $\dot{\gamma}/\dot{\varepsilon}$ ratios as indicated. The simple shear direction is 45°→280°, as in the mylonite zone (domain 3). The maximum stretching direction of the pure shearing component is parallel to the strike of the shear zone boundary (00°→280°) and the maximum shortening direction is perpendicular to the shear zone boundary (00°→010°). (c) Stretch of the lineation and stretch along the strike of the shear zone boundary, for selected points along triclinic rotation paths as indicated with symbols in (b) and (c). Also indicated is the strain intensity, S, defined by Ramsay and Huber (1983, pp. 201–202) as: $S = \sqrt{\left(\frac{(\lambda_1)^{\frac{1}{2}}}{(\lambda_2)^{\frac{1}{2}}} - 1\right)^2 + \left(\frac{(\lambda_2)^{\frac{1}{2}}}{(\lambda_3)^{\frac{1}{2}}} - 1\right)^2}$.

most consistent with a simple shear flow pattern, or triclinic flow with a high $\dot{\gamma}/\dot{\varepsilon}$ ratio and relatively low strain. If flow was truly simple shear, then the question arises why there would not be a pure shearing component if there is one adjacent to the mylonite zone. Intuitively, there appears to be a strain compatibility problem if the mylonite zone would not experience strike-parallel stretching and shear zone-normal shortening while the country rocks do. For this reason, triclinic flow with dextral, north-side-up shear and shear zone boundary-parallel horizontal stretching and shear zone-normal shortening, rather than simple shearing, is likely to have occurred in domain 3. As long as the $\dot{\gamma}/\dot{\varepsilon}$ ratio is high and the strain is low enough that lineations and fold hinge lines have not rotated away from the shear direction, then the rotation patterns (Figs. 7 and 9b) are consistent with the observed orientations of lineations and fold hinge lines (Fig. 8). To test whether this is a reasonable explanation, we calculated finite strains (stretches) of fold hinge lines, lineations and the shear zone boundary for various points along the rotation paths (Figs. 7 and 9b).

4.3. Finite stretch

If flow in domain 3 included a pure shearing component with the same symmetry as the pure shearing in domain 4, then flow in domain 3 was triclinic. For low finite strains, and high $\dot{\gamma}/\dot{\varepsilon}$ ratios, triclinic flow paths are similar to monoclinic flow paths. For example, λ_1 follows a rotation path close to the vorticity-normal section (VNS) towards the shear direction (Fig. 9b). In theory, at higher strains, the lineations would rotate away from the VNS towards the fabric attractor (Jiang and Williams, 1998), but the finite strain may be too high for that to occur in nature, as explained below. For the pre-existing fold hinge lines with orientation 60° → 140° to rotate towards an orientation close to the shear direction (45° → 280°), the finite stretch of that fold hinge line would be ~5.3 and the shear zone boundary-parallel horizontal stretch ~2.1 (Fig. 7). Fig. 9b shows the orientations of stretching lineations as they would initiate and rotate during triclinic flow, using the same parameters as above. For a lineation to rotate towards an orientation close to the shear direction with $\dot{\gamma}/\dot{\varepsilon} = 20$, the stretch along that lineation would be ~6.6 and the shear zone boundary-parallel horizontal stretch would be ~1.4 (Fig. 9c). Thus, it is likely for both pre-existing fold hinge lines and lineations, and newly formed stretching lineations, to rotate towards the shear direction. However, rotation beyond the shear direction towards horizontal orientations (the fabric attractor) would require much higher finite stretches. For example, the open diamond in Fig. 9b requires a stretch along the lineation of 34.9 (Fig. 9c). Fold hinge lines and lineations may be obliterated due to strong deformation or become hard recognize or measure. Furthermore, at such high strains, it is likely that rotated lineations recrystallize and a new lineation forms (cf. Means, 1981 (steady-state foliation); Jiang and Williams, 1998). For those reasons, the high-strain part of the rotation paths for lineations and fold hinge lines may not be recorded in nature and only the low-strain part may be relevant. These low-strain parts of rotation paths for triclinic flow with high $\dot{\gamma}/\dot{\varepsilon}$ ratios may be indistinguishable from monoclinic flow patterns. Thus, despite the apparent monoclinic symmetry of fabrics in domain 3, flow may have been triclinic with a high $\dot{\gamma}/\dot{\varepsilon}$ ratio.

The magnitude of shear zone boundary-parallel horizontal stretch is best constrained by the pure shearing model and domain 4. In the pure shearing model (Fig. 7, $\dot{\gamma}/\dot{\varepsilon} = 0$), the finite stretch along the strike of the shear zone needs to be ~9.5 for the pre-existing fold hinge lines with orientation 60°→140° to rotate to a subhorizontal orientation (as observed in domain 4; Fig. 8b). The feasibility of such a high strike-parallel stretch is discussed below.

4.4. Shear zone boundary-parallel horizontal stretch

The discussion above leads to the general question of how much shear zone boundary-parallel horizontal stretch and shear zone-orthogonal shortening is likely to occur in nature. While shear zone boundary-parallel horizontal stretch has been documented in the literature, this stretch is more commonly a result of the simple shearing component than the pure shearing component (e.g. Goscombe and Gray, 2003; Pereira et al., 2008) and not truly parallel to the shear zone boundary. The difference between the two types of stretch is illustrated in Fig. 10. Both figures show transpression, one with a high simple shearing component ($\dot{\gamma}/\dot{\varepsilon} = 20$, Fig. 10a) and one with a high pure shearing component ($\dot{\gamma}/\dot{\varepsilon} = 0.1$, Fig. 10b). The stretch in Fig. 10a is mostly as a result of simple shear and not truly parallel to the shear zone boundary. While the maximum stretch is 10.57, the shear zone-parallel stretch is only 1.65. Fig. 10b shows a high shear zone-parallel stretch as a result of pure shear. Because the simple shearing component is very low, the maximum stretch (7.40) is nearly the same as the shear zone-parallel stretch (7.39). The type of stretch in Fig. 10a is common for shear zones with large displacements. Displacements, shear strains and associated stretches can be high, because simple shearing is a strain softening process (Williams and Price, 1990; Lin et al., 1998). On the contrary, the amount of shear zone-parallel stretch as a result of a pure shearing component (Fig. 10b) is limited,

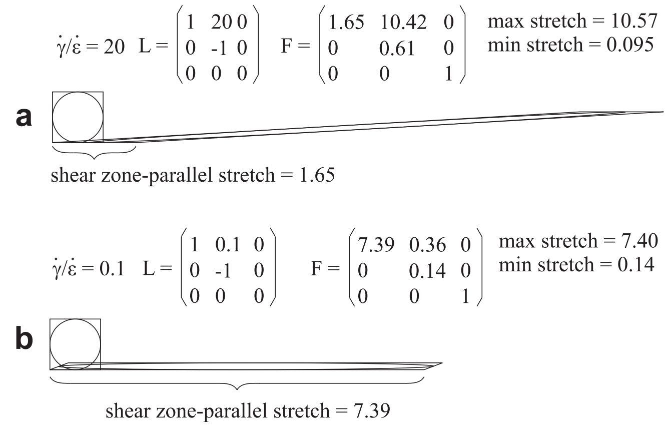

Fig. 10. Two dimensional models of transpression zones with $\dot{\gamma}/\dot{\varepsilon} = 20$ (a) and $\dot{\gamma}/\dot{\varepsilon} = 0.1$ (b). The stretch in (a) is mostly as a result of simple shearing and not truly parallel to the shear zone boundary. The stretch in (b) is mostly a result of a pure shear stretch parallel to the shear zone boundary.

because pure shearing is a strain hardening process (Williams and Price, 1990; Lin et al., 1998). Shear zone-parallel stretch also leads to space problems, and to strain incompatibility problems between the shear zone and adjacent rocks (Vitale and Mazzoli, 2008). Therefore, shear zone-parallel stretch is more commonly vertical or oblique (Tikoff and Greene, 1997; Lin et al., 1998; Czeck and Hudleston, 2003) and not constrained by space.

Large shear zone boundary-parallel horizontal stretches are known to occur in horizontal shear zones, such as channel flow and infrastructure zones (Beaumont et al., 2006; Culshaw et al., 2006; Hodges, 2006; Kuiper et al., 2006; Williams et al., 2006; Vitale and Mazzoli, 2009). Shear zone boundary-parallel horizontal stretch in steep transpression zones is not as common and not likely to be high (e.g. Pulver et al., 2002; Fügenschuh and Schmid, 2005; Jeřábek et al., 2007). Such transpression zones may exist in zones of oblique convergence, in orogens with an orogen-parallel stretch component. The maximum amount of orogen-parallel stretch during convergence is not well quantified in the literature, but current estimates are low (cf. Fügenschuh and Schmid, 2005; Jeřábek et al., 2007). In the West Carpathians, Jeřábek et al. (2007) estimated an orogen-parallel stretch of up to ∼1.8, based on the shape of recrystallized quartz aggregates. While these are minimum estimates for stretch, no evidence for higher syn-orogenic orogen-parallel stretch is currently documented in the literature.

One setting where higher shear zone boundary-parallel horizontal stretches in subvertical shear zones may exist is in escape-tectonic settings, where shear zone boundary-parallel horizontal stretch and orogen-parallel stretch is a result of lateral extrusion. In escape tectonics, relatively rigid blocks are laterally extruded in a direction parallel to the orogen along discrete faults (e.g. Molnar and Tapponnier, 1975; Jacobs and Thomas, 2004). At shallow levels, this explains large-scale orogen-parallel stretch, but the individual faults or shear zones do not necessarily stretch. However, at depth, lateral extrusion may occur in a more homogeneous manner (cf. Yang and Liu, 2009), so that shear zones between the laterally extruded blocks are stretched. The Aiken River shear zone may be an example, as discussed in Kuiper et al. (in review).

5. Conclusions

The ARSZ shows evidence for triclinic transpression. Along the ARSZ, triclinic transpression is partitioned into an apparent simple shearing domain and an apparent pure shearing domain. A 1–1.5 km wide central mylonite zone (domain 3) shows an apparent monoclinic dextral, north-side-up simple shearing symmetry, but the actual flow is interpreted as triclinic with a high $\dot{\gamma}/\dot{\varepsilon}$ ratio. To the north of this zone, a 1–1.5 km transitional zone (domain 4) exists with apparent pure shearing symmetry (involving shear zone boundary-parallel horizontal stretch and shear zone-normal shortening), but the flow may have been triclinic with a low $\dot{\gamma}/\dot{\varepsilon}$ ratio. Thus, in triclinic transpression zones, flow can be partitioned into apparent monoclinic and orthorhombic domains even though the true flow in these domains may have been triclinic.

The boundary between domains 4 and 5 is transitional and in domain 5 the shear zone boundary-parallel horizontal stretch and shear zone-orthogonal shortening are not as pronounced as in domain 4. Domain 6 shows evidence of weak shear zone-orthogonal shortening, as far as ∼20 km north of the ARSZ. Thus, the simple shearing is concentrated in a narrow zone with sharp boundaries, while pure shearing is distributed over a broad zone with diffuse boundaries (cf. Fig. 3 of Lin et al., 2007). This is consistent with simple shearing being a softening process and pure shearing being a hardening process (cf. Williams and Price, 1990; Lin et al., 1998). In the ARSZ, the width of the zone affected by pure shearing is about three times the width of the zone affected by simple shearing.

The shear zone boundary-parallel horizontal stretch of the ARSZ is in the order of 10, based on results of domain 4. In domain 3 the shear zone boundary-parallel horizontal stretch is difficult to estimate, because of the high $\dot{\gamma}/\dot{\varepsilon}$ ratio and high strains associated with the simple shear components. The shear zone boundary-parallel horizontal stretch of ∼10 along the ARSZ is most likely to have occurred in an escape-tectonic setting.

Acknowledgements

We thank the Manitoba Geological Survey, and especially Christian Böhm and Tim Corkery, for logistical field support and scientific discussion. This project was further supported by Manitoba Hydro, an NSERC grant and support from the China Changjiang Scholars Program to Shoufa Lin, and an NSERC Discovery Grant and a China National Science Foundation Grant (NSFC 40828001) to Dazhi Jiang.The journal reviewers, Scott Giorgis and Pedro Oyhantçabal, are thanked for their comments. We are grateful to Paul Williams who contributed to our careers and continues to inspire us all.

References

Ansdell, K.M., 2005. Tectonic evolution of the Manitoba–Saskatchewan segment of the Paleoproterozoic Trans-Hudson orogen, Canada. Canadian Journal of Earth Sciences 42, 741–759.

Beaumont, C., Nguyen, M.H., Jamieson, R.A., Ellis, S., 2006. Crustal flow modes in large hot orogens. In: Law, R.D., Searle, M., Godin, L. (Eds.), Channel Flow, Ductile Extrusion and Exhumation of Lower-mid Crust in Continental Collision Zones. Geological Society, London, Special Publications, vol. 268, pp. 91–145.

Böhm, C.O., Hartlaub, R.P., Heaman, L.M., 2007. The Assean Lake complex: ancient crust at the northwestern margin of the Superior craton, Manitoba, Canada. In: Van Kranendonk, M.J., Smithies, R.H., Bennett, V.C. (Eds.), Earth's Oldest Rocks. Developments in Precambrian Geology, vol. 15, pp. 751–773.

Böhm, C.O., Heaman, L.M., Corkery, M.T., 1999. Archean tectonic evolution of the northwestern Superior craton margin: U–Pb zircon results from the Split Lake Block. Canadian Journal of Earth Sciences 36, 1973–1987.

Böhm, C.O., Heaman, L.M., Creaser, R.A., Corkery, M.T., 2000. Discovery of pre-3.5 Ga exotic crust at the northwestern Superior Province margin, Manitoba. Geology 28, 75–78.

Böhm, C.O., Heaman, L.M., Stern, R.A., Corkery, M.T., Creaser, R.A., 2003. Nature of Assean Lake ancient crust, Manitoba: a combined SHRIMP–ID-TIMS U–Pb geochronology and Sm–Nd isotope study. Precambrian Research 126, 55–94.

Corkery, M.T., 1985. Geology of the Lower Nelson River Project area. Manitoba Energy and Mines, Geological Report GR82-1, 66 p.

Corrigan, D., Hajnal, Z., Németh, B., Lucas, S.B., 2005. Tectonic framework of a Paleoproterozoic arc – continent to continent – continent collisional zone, Trans-Hudson Orogen, from geological and seismic reflection studies. Canadian Journal of Earth Sciences 42, 421–434.

Culshaw, N.G., Beaumont, C., Jamieson, R.A., 2006. The orogenic superstructure-infrastructure concept: revisited, quantified, and revived. Geology 34, 733–736.
Czeck, D.M., Hudleston, P.J., 2003. Testing for obliquely plunging lineations in transpression: a natural example and theoretical discussion. Journal of Structural Geology 25, 959–982.
Downey, M.W., Lin, S., Böhm, C.O., Rayner, N.M., 2009. Timing and kinematics of crustal movement in the northern Superior superterrane: insights from the Gull Rapids area of the Split Lake block, Manitoba. Precambrian Research 168, 134–148.
Fügenschuh, B., Schmid, S.M., 2005. Age and significance of core complex formation in a very curved orogen: evidence from fission track studies in the South Carpathians (Romania). Tectonophysics 404, 33–53.
Goscombe, B., Gray, D., 2003. Structure and strain variation at mid-crustal levels in a transpressional orogen: a review of Kaoko Belt structure and the character of West Gondwana amalgamation and dispersal. Gondwana Research 12, 45–85.
Hartlaub, R.P., Heaman, L.M., Simonetti, A., Böhm, C.O., 2006. Relicts of Earth's earliest crust, U-Pb, Lu-Hf, and morphological characteristics of >3.7 Ga detrital zircon of the western Canadian Shield. In: Reimold, W.U., Gibson, R.L. (Eds.), Processes on the Early Earth. Geological Society of America, Special Paper, vol. 405, pp. 75–89.
Hartlaub, R.P., Böhm, C.O., Kuiper, Y.D., Bowerman, M.S., Heaman, L.M., 2004. Archean and Paleoproterozoic geology of the northwestern Split Lake Block, Superior Province, Manitoba (parts of NTS 54D4, 5, 6 and 64A1). Manitoba Industry, Economic Development and Mines, Manitoba Geological Survey, Report of Field Activities 2004, pp. 187–194.
Haugh, I., 1969. Geology of the Split Lake Area. Manitoba Mines and Natural Resources, Mines Branch, Publication 65-2, 87 p.
Hodges, K.V., 2006. A synthesis of the Channel Flow-Extrusion hypothesis as developed for the Himalayan-Tibetan orogenic system. In: Law, R.D., Searle, M., Godin, L. (Eds.), Channel Flow, Ductile Extrusion and Exhumation of Lower-mid Crust in Continental Collision Zones. Geological Society, London, Special Publications, vol. 268, pp. 71–90.
Hulbert, L.J., Hamilton, M.A., Horan, M.F., Scoates, R.F.J., 2005. U–Pb zircon and Re–Os isotope geochronology of Mineralized ultramafic Intrusions and associated Nickel Ores from the Thompson Nickel belt, Manitoba, Canada. Economic Geology 100, 29–41.
Jacobs, J., Thomas, R.J., 2004. Himalayan-type indenter-escape tectonics model for the southern part of the late Neoproterozoic–early Paleozoic East African–Antarctic orogen. Geology 32, 721–724.
Jeřábek, P., Stünitz, H., Heilbronner, R., Lexa, O., Schulmann, K., 2007. Microstructural-deformation record of an orogen-parallel extension in the Vepor Unit, West Carpathians. Journal of Structural Geology 29, 1722–1743.
Jeffery, G.B., 1922. The motion of ellipsoidal particles immersed in a viscous fluid. Proceedings of the Royal Society of London A 102, 161–179.
Jiang, D., 2007a. Numerical modeling of the motion of rigid ellipsoidal objects in slow viscous flows: a new approach. Journal of Structural Geology 29, 189–200.
Jiang, D., 2007b. Sustainable transpression: an examination of strain and kinematics in deforming zones with migrating boundaries. Journal of Structural Geology 29, 1984–2005.
Jiang, D., Williams, P.F., 1998. High-strain zones: a unified model. Journal of Structural Geology 20, 1105–1120.
Jiang, D., Williams, P.F., 1999. When do dragfolds not develop into sheath folds in shear zones? Journal of Structural Geology 21, 577–583.
Jiang, D., Lin, S., Williams, P.F., 2001. Deformation path in high-strain zones, with reference to slip partitioning in transpressional plate-boundary regions. Journal of Structural Geology 23, 991–1005.
Kuiper, Y.D., Williams, P.F., Kruse, S., 2006. Possibility of channel flow in the southern Canadian Cordillera: a new approach to explain existing data. In: Law, R.D., Searle, M., Godin, L. (Eds.), Channel Flow, Ductile Extrusion and Exhumation of Lower-mid Crust in Continental Collision Zones. Geological Society, London, Special Publications, vol. 268, pp. 587–609.
Kuiper, Y.D., Jiang, D., Lin, S., 2007. Relationship between non-cylindrical fold geometry and the shear direction in monoclinic and triclinic shear zones. Journal of Structural Geology 29, 1022–1033.
Kuiper, Y.D., Lin, S., Jiang, D., 2009. Deformation partitioning in transpressional shear zones: an example from the Superior Boundary Zone, Manitoba, Canada. Eos Transactions, American Geophysical Union, 90(22), Joint Assembly Supplements, Abstract GA22A-07.
Kuiper, Y.D., Lin, S., Böhm, C.O. Himalayan-style escape tectonics along the Superior Province margin in Manitoba, Canada. Precambrian Research, in review.
Kuiper, Y.D., Lin, S., Böhm, C.O., Corkery, M.T., 2003. Structural geology of the Assean Lake and Aiken River deformation zones, northern Manitoba (NTS 64A1, 2 and 8). In: Report of Activities 2003, Manitoba Industry, Economic Development and Mines, Manitoba Geological Survey, pp. 105–113.
Kuiper, Y.D., Lin, S., Böhm, C.O., Corkery, M.T., 2004a. Structural geology of Assean Lake, northern Manitoba (NTS 64A1, 2, 8). In: Report of Activities 2004, Manitoba Industry, Economic Development and Mines, Manitoba Geological Survey, pp. 195–200.
Kuiper, Y.D., Lin, S., Böhm, C.O., Corkery, M.T., 2004b. Structural geology of the Aiken River deformation zone, northern Manitoba (NTS 64A1, 2). In: Report of Activities 2004, Manitoba Industry, Economic Development and Mines, Manitoba Geological Survey, pp. 201–208.
Lin, S., Jiang, D., Williams, P.F., 1998. Transpression (or transtension) zones of triclinic symmetry: natural example and theoretical modeling. In: Holdsworth, R.E., Strachan, R.A., Dewey, J.F. (Eds.), Continental Transpressional and Transtensional Tectonics. Geological Society, London, Special Publication, vol. 135, pp. 41–57.
Lin, S., Jiang, D., Williams, P.F., 2007. Importance of differentiating ductile slickenside striations from stretching lineations and variation of shear direction across a high-strain zone. Journal of Structural Geology 29, 850–862.
Machado, N., 1990. Timing of collisional events in the Trans-Hudson orogen: evidence from U-Pb geochronology for the New Quebec orogen, the Thompson belt and the Reindeer zone (Manitoba and Saskatchewan). In: Lewry, J.F., Stauffer, M.R. (Eds.), The Early Proterozoic Trans-Hudson Orogen of North America. Geological Association of Canada, Special Paper, vol. 37, pp. 433–441.
Machado, N., Krogh, T.E., Weber, W., 1990. U–Pb geochronology of the Thompson Belt (Manitoba): evidence for pre-Kenoran and Pikwitonei-type crust and early Proterozoic basement reactivation in the western margin of the Archean Superior Province. Canadian Journal of Earth Sciences 27, 794–802.
Means, W.D., 1981. The concept of steady-state foliation. Tectonophysics 78, 179–199.
Means, W.D., 1990. Kinematics, stress, deformation and material behavior. Journal of Structural Geology 12, 953–971.
Mezger, K., Bohlen, S.R., Hanson, G.N., 1990. Metamorphic history of the Archean Pikwitonei granulite domain and the Cross Lake Subprovince, Superior Province, Manitoba, Canada. Journal of Petrology 31, 483–517.
Molnar, P., Tapponnier, P., 1975. Cenozoic tectonics of Asia; effects of a continental collision. Science 189, 419–426.
Percival, J.A., 2007. Eo- to Mesoarchean terranes of the Superior Province and their tectonic context. In: Van Kranendonk, M.J., Smithies, R.H., Bennett, V.C. (Eds.), Earth's Oldest Rocks. Developments in Precambrian Geology, Vol. 15, pp. 1065–1085.
Pereira, M.F., Apraiz, A., Silva, J.B., Chichorro, M., 2008. Tectonothermal analysis of high-temperature mylonitization in the Coimbra–Córdoba shear zone (SW Iberian Massif, Ouguela tectonic unit, Portugal): evidence of intra-continental transcurrent transport during the amalgamation of Pangea. Tectonophysics 461, 378–394.
Pulver, M.H., Crespi, J.M., Byrne, T.B., 2002. Lateral extrusion in a transpressional collision zone: an example from the pre-Tertiary metamorphic basement of Taiwan. In: Byrne, T.B., Liu, C.-S. (Eds.), Geology and Geophysics of an Arc-Continent Collision, Taiwan. Geological Society of America, Special Paper, vol. 358, pp. 107–120.
Ramsay, J.G., Huber, M.I., 1983. The Techniques of Modern structural geology. In: Strain Analysis, vol. 1. Academic Press, San Diego.
Robin, P.-Y.F., Cruden, A.R., 1994. Strain and vorticity patterns in ideally ductile transpression zones. Journal of Structural Geology 16, 447–466.
Sanderson, D.J., Marchini, W.R.D., 1984. Transpression. Journal of Structural Geology 6, 449–458.
Tikoff, B., Greene, D., 1997. Stretching lineations in transpressional shear zones. Journal of Structural Geology 19, 29–40.
Vitale, S., Mazzoli, S., 2009. Finite strain analysis of a natural ductile shear zone in limestones; insights into 3-D coaxial vs. non-coaxial deformation partitioning. Journal of Structural Geology 31, 104–113.
Vitale, S., Mazzoli, S., 2008. Heterogeneous shear zone evolution: the role of shear strain hardening/softening. Journal of Structural Geology 30, 1383–1395.
Williams, P.F., Price, G.P., 1990. Origin of kinkbands and shear-band cleavage in shear zones: an experimental study. Journal of Structural Geology 12, 145–164.
Williams, P.F., Jiang, D., Lin, S., 2006. Interpretation of deformation fabrics of infrastructure zone rocks in the context of channel flow and other models. In: Law, R.D., Searle, M., Godin, L. (Eds.), Channel Flow, Ductile Extrusion and Exhumation of Lower-mid Crust in Continental Collision Zones. Geological Society, London, Special Publications, vol. 268, pp. 221–235.
Yang, Y., Liu, M., 2009. Crustal thickening and lateral extrusion during the Indo-Asian collision; a 3D viscous flow model. Tectonophysics 465, 128–135.
Zwanzig, H.V., 2005. Hot, thin and mineral-rich—evolution of the Paleoproterozoic Trans-Hudson Orogen in western Canada. Abstract and oral presentation for 2004 Robinson Lecture Tour. Manitoba Geological Survey, Manitoba Industry, Economic Development and Mines.
Zwanzig, H.V., Macek, J.J., McGregor, C.R., 2007. Lithostratigraphy and Geochemistry of the high-grade metasedimentary rocks in the Thompson Nickel Belt and adjacent Kisseynew domain, Manitoba: implications for Nickel Exploration. Economic Geology 102, 1197–1216.